

# RSC Advances



This is an *Accepted Manuscript*, which has been through the Royal Society of Chemistry peer review process and has been accepted for publication.

*Accepted Manuscripts* are published online shortly after acceptance, before technical editing, formatting and proof reading. Using this free service, authors can make their results available to the community, in citable form, before we publish the edited article. This *Accepted Manuscript* will be replaced by the edited, formatted and paginated article as soon as this is available.

You can find more information about *Accepted Manuscripts* in the [Information for Authors](#).

Please note that technical editing may introduce minor changes to the text and/or graphics, which may alter content. The journal's standard [Terms & Conditions](#) and the [Ethical guidelines](#) still apply. In no event shall the Royal Society of Chemistry be held responsible for any errors or omissions in this *Accepted Manuscript* or any consequences arising from the use of any information it contains.



Journal Name

ARTICLE

## A fast-response, fluorescent 'turn-on' chemosensor for selective detection of Cr<sup>3+</sup>

Received 00th January 20xx,  
Accepted 00th January 20xx

DOI: 10.1039/x0xx00000x

www.rsc.org/

Chunhua Fan<sup>a</sup>, Ximing Huang<sup>a</sup>, Cory A. Black<sup>b</sup>, Xingxing Shen<sup>c</sup>, Junjie Qi<sup>a</sup>, Yuanping Yi<sup>c</sup>, Zhengliang Lu<sup>a,\*</sup>, Yong Nie, Guoxin Sun<sup>a,\*</sup>

A fast-response, highly selective and sensitive chemosensor, **3**, for Cr<sup>3+</sup> detection with turn-on fluorescence behavior in the physiological pH range was designed and synthesized. The chemosensor contained a combined push-pull system in which the fluorescent phenanthro[9,10-*d*]oxazole moiety acts as both the electron donor and a potential binding site. An electron deficient nitrile group served as the electron acceptor. A significant enhancement of fluorescence emission intensities was observed with increasing Cr<sup>3+</sup> concentration upon excitation at 300 nm. The emission intensity reached its maximum on adding 8 equiv. of Cr<sup>3+</sup> where the quantum yield of **3**-Cr<sup>3+</sup> was found to be 0.917, ca. 7-fold larger than the chemosensor **3**. The selectivity mechanism of **3** for Cr<sup>3+</sup> was found to be based on the combined effects of the inhibition of ICT and CHEF. Remarkably the entire process was virtually complete in only 10 seconds, with a minimum detection limit for Cr<sup>3+</sup> of 1.72 × 10<sup>-8</sup> M<sup>-1</sup>.

### Introduction

Fast-response sensors for detection of heavy and transition metal ions have been attracting considerable attention due to their potential application in biological and environmental systems.<sup>1-4</sup> As one of the essential micronutrients in the human body, the trivalent form of chromium, Cr<sup>3+</sup>, plays a crucial role in effectively maintaining the metabolism of carbohydrates, adipose cells and proteins.<sup>5</sup> However, Cr<sup>3+</sup> deficiency within biological systems adversely increases the risk of maturity-onset diabetes, cardiovascular diseases and nervous system disorders. High levels of Cr<sup>3+</sup> can negatively affect cellular structures and damage cellular components by forming reactive oxygen species.<sup>6-8</sup> Furthermore, the use of chromium in common industrial processes such as, dyes and paints manufacturing, alloy production and metallurgy also engenders serious environmental pollution as Cr<sup>3+</sup> could be converted to the more toxic Cr<sup>6+</sup> by redox cycling.<sup>9,10</sup> Thus from a health and environmental point of view, it is urgent to develop highly selective chemosensors for Cr<sup>3+</sup> detection. At present, the fluorescence spectroscopy for trace Cr<sup>3+</sup> detection is an effective method due to its high sensitivity and selectivity, operational simplicity for real-time imaging. In contrast, traditional analytical techniques such as atomic absorption/emission spectroscopy of inductively coupled plasma mass spectrometry are less effective.<sup>11,12</sup> There are many literature reports of chemosensors that have been designed to make use of the turn-off

mechanism which involves paramagnetic luminescence quenching of the Cr<sup>3+</sup> fluorophore.<sup>13-15</sup> Great efforts have also been made on designing turn-on sensors because turn-off sensors tend to produce a low signal output upon binding and are therefore prone to interfere with the temporal separation of similar complexes with time-resolved fluorometry.<sup>16-19</sup> Unfortunately, most turn-on chemosensors for detection of Cr<sup>3+</sup> have focused on rhodamine derivatives, which can probe Cr<sup>3+</sup> by conversion of the non-fluorescent rhodamine spirolactam to the highly fluorescent ring-open amide form upon binding.<sup>20-25</sup> Furthermore, the long equilibrium time and high limits of detection of rhodamine derivatives do not satisfy the requirement of fast-response and high sensitivity under pharmacological conditions. The limitations of rhodamine-based chemosensors have therefore inspired us to develop novel fast-response, highly selective and sensitive chemosensors for Cr<sup>3+</sup> detection.

A number of different mechanisms, including intramolecular charge transfer (ICT), chelation enhanced fluorescence (CHEF) and fluorescence resonance energy transfer (FRET), have been extensively used to design fluorescent turn-on chemosensors. We envisioned that combination of ICT and CHEF mechanisms could be simultaneously applied to construct fluorescence turn-on sensors of Cr<sup>3+</sup>. Usually ICT will take place upon excitation of a molecule containing both an electron rich group and an electron deficient group. CHEF could turn on or off intramolecular charge transfer from the donor to the acceptor, which thereby affects the fluorescence emission intensity of the fluorophore. Based on our speculation above and continuation of our work, we herein describe the design and synthesis of a novel fluorescent probe 3'-(1H-phenanthro[9,10-*d*]imidazol-2-yl)-4'-(pyridin-2-ylmethoxy)-[1,1'-biphenyl]-4-carbonitrile (**3**) which displays a fast fluorescent turn-on response to Cr<sup>3+</sup>. Sensor **3** contains a combined push-pull system in which the fluorescent phenanthro[9,10-*d*]oxazole moiety not only acts as the electron donor but also provides a potential binding site for Cr<sup>3+</sup>. 3'-formyl-4'-(pyridin-2-ylmethoxy)biphenyl-4-carbonitrile was chosen

<sup>a</sup> School of Chemistry and Chemical Engineering, University of Jinan, Jinan 250022, P. R. China. E-Mail: zhenqiang.lu@yahoo.com

<sup>b</sup> The Australian Wine Research Institute, P.O. Box 197, Glen Osmond, South Australia 5064, Australia

<sup>c</sup> Beijing National Laboratory for Molecular Sciences, CAS Key Laboratory of Organic Solids, Institute of Chemistry, Chinese Academy of Sciences, Beijing 100190, China.

† Electronic Supplementary Information (ESI) available. See DOI: 10.1039/x0xx00000x

as the electron acceptor and the potential chelating unit, in which the an electron deficient CN group is able to promote ICT. As anticipated, sensor **3** gives a fast turn-on response for Cr<sup>3+</sup> detection after only 10 seconds.

## Experimental

### Materials and instruments

All solvents were purified using standard methods. All starting materials were used as received. <sup>1</sup>H and <sup>13</sup>C NMR were performed on a 400 MHz/100 MHz Bruker Advance DRX 400 spectrometer. High resolution mass measurements were carried out on a Waters-Q-TOF-Premier (ESI) or a Shimadzu LCMS-IT-TOF (ESI). Elemental analysis (C, H and N) was carried out using a Perkin-Elmer 4100 elemental analyzer. UV-Vis absorption spectra were measured on a Shimadzu UV-2100 spectrophotometer. Fluorescence spectra were obtained on an F-380 spectrofluorophotometer.

### Synthesis of 3'-formyl-4'-hydroxybiphenyl-4-carbonitrile (1)

Compound **1** was synthesized according to a modified procedure.<sup>26, 27</sup> Dry paraformaldehyde (6.6 g) was added to a mixture of 4'-hydroxybiphenyl-4-carbonitrile (3.1 g, 16 mmol), triethylamine (8.4 mL, 61 mmol) and anhydrous MgCl<sub>2</sub> (2.3 g, 24 mmol) in dry acetonitrile (50 mL). The mixture was heated to reflux for 6 h, and then cooled to room temperature, acidified with 1M HCl, and extracted with ethyl acetate (3 × 20 mL). The combined organic layer was washed with water and dried over MgSO<sub>4</sub>. The crude material was purified by column chromatography to give 1.95 g of the title compound as a white solid in a 55% yield. <sup>1</sup>H NMR (400 MHz, CDCl<sub>3</sub>) δ ppm: 11.11 (s, 1H), 9.99 (s, 1H), 7.73-7.78 (m, 4H), 7.66 (dt, *J* = 8.59, 2.12 Hz, 2H), 7.12 (d, *J* = 8.37 Hz, 1H). <sup>13</sup>C NMR (100 MHz, CDCl<sub>3</sub>) δ ppm: 196.4555, 161.9312, 135.5569, 132.8403, 132.2187, 127.1455, 120.8202, 111.0172, 77.4160, 77.0977, 76.7798. HRMS (ESI<sup>+</sup>, Fig. S3) calc. for C<sub>19</sub>H<sub>13</sub>NO<sub>2</sub> (M + H<sup>+</sup>) 223.0633, found 223.0734.

### Synthesis of 3'-formyl-4'-(pyridin-2-ylmethoxy)biphenyl-4-carbonitrile (2)

**2** (1.1 g, 5 mmol), 2-(chloromethyl)pyridine hydrochloride (0.82 g, 5 mmol), anhydrous potassium carbonate (3.5 g, 25 mmol) and potassium iodide (0.42 g, 2.5 mmol) were dissolved in dry acetonitrile (35 mL). The mixture was refluxed for 6 h, cooled to room temperature and filtered. The filtrate was washed with ethyl acetate (3 × 20 mL), dried over MgSO<sub>4</sub> and the solvent was removed under reduced pressure. The crude product was purified by column chromatography to afford 0.8 g of the pure product as a yellow solid in 51% yield. <sup>1</sup>H NMR (400 MHz, CDCl<sub>3</sub>) δ ppm: 10.65 (s, 1H), 8.64 (d, *J* = 5.57 Hz, 1H), 8.11 (d, *J* = 2.51 Hz, 1H), 7.76-7.78 (m, 2H), 7.72 (d, *J* = 8.34 Hz, 2H), 7.67 (d, *J* = 8.60 Hz, 2H), 7.55 (d, *J* = 7.82 Hz, 1H), 7.30 (dd, *J* = 7.34, 5.10 Hz, 1H), 7.18 (d, *J* = 8.75 Hz, 1H), 5.40 (s, 2H). <sup>13</sup>C NMR (100 MHz, CDCl<sub>3</sub>) δ ppm: 189.1033, 160.8735, 155.8735, 149.5142, 143.7822, 137.1566, 134.3457, 125.3517, 123.1937, 121.4113, 113.9511, 111.0266, 71.4160. Anal. calc. for C<sub>20</sub>H<sub>14</sub>N<sub>2</sub>O<sub>2</sub>: C, 76.42; H, 4.49; N, 8.91; found: C, 76.38; H, 4.52; N, 8.95.

### Synthesis of 3'-(1H-phenanthro[9,10-d]imidazol-2-yl)-4'-(pyridin-2-ylmethoxy)-[1,1'-biphenyl]-4-carbonitrile (3)

A mixture of 9,10-phenanthrenequinone (0.042 g, 0.2 mmol) and ammonium acetate (0.15 g, 2 mmol) was suspended in a solution of ethanol (15 mL) and dichloromethane (1.5 mL). The suspension was heated to reflux until all solids were dissolved and then cooled to room temperature. **3**

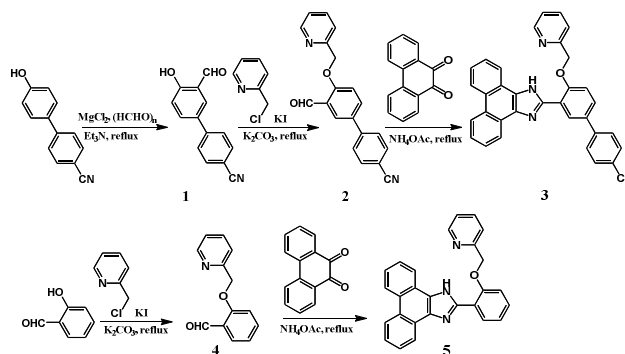
(0.063 g, 0.2 mmol) and a drop of acetic acid were added to the mixture, which was again heated to reflux for 2 h, cooled, and the crude product was filtered and washed with ethanol to afford 0.045 g of compound **3** (0.045 g, 45%) as a light yellow solid. <sup>1</sup>H NMR (400 MHz, CDCl<sub>3</sub>) δ ppm: 12.98 (s, 1H), 9.00 (t, *J* = 5.69 Hz, 2H), 8.84 (d, *J* = 7.59 Hz, 1H), 8.79 (d, *J* = 8.26 Hz, 1H), 8.74 (d, *J* = 8.26 Hz, 1H), 8.40 (d, *J* = 7.78 Hz, 1H), 7.75-7.85 (m, 6H), 7.73 (d, *J* = 4.93 Hz, 1H), 7.67 (d, *J* = 7.78 Hz, 2H), 7.60 (dd, *J* = 8.70, 2.42 Hz, 1H), 7.42-7.48 (m, 2H), 7.24 (d, *J* = 8.46 Hz, 1H), 5.53 (s, 2H). <sup>13</sup>C NMR (100 MHz, CDCl<sub>3</sub>) δ ppm: 155.4558, 155.3922, 149.9561, 146.5190, 144.5912, 137.1551, 132.5776, 127.4694, 123.5267, 121.5182, 121.3903, 119.0652, 113.3245, 110.6370, 70.5648. HRMS (ESI<sup>+</sup>, Fig. S8) calc. for C<sub>34</sub>H<sub>22</sub>N<sub>4</sub>O (M + H<sup>+</sup>) 503.1866, found 503.1894.

### Synthesis of 2-(pyridin-2-ylmethoxy)benzaldehyde (4)

Compound **4** was synthesized using the same procedure as compound **2** (0.671 g, 31.5%). <sup>1</sup>H NMR (400 MHz, CDCl<sub>3</sub>) δ ppm: 10.61 (s, 1H), 8.60 (d, *J* = 4.74 Hz, 1H), 7.85 (d, *J* = 7.76 Hz, 1H), 7.74 (td, *J* = 7.78, 1.81 Hz, 1H), 7.49-7.56 (m, 2H), 7.25 (t, *J* = 5.04 Hz, 1H), 7.05 (t, *J* = 7.82 Hz, 2H), 5.31 (s, 2H). <sup>13</sup>C NMR (100 MHz, CDCl<sub>3</sub>) δ ppm: 189.5491, 160.5508, 156.2593, 149.3338, 137.0619, 136.0331, 128.7990, 125.0443, 122.9736, 121.2581, 112.9863, 70.9946. Anal. calc. for C<sub>13</sub>H<sub>11</sub>NO<sub>2</sub>: C, 73.23; H, 5.20; N, 6.57; found: C, 73.28; H, 5.15; N, 6.61.

### Synthesis of 2-(2-(pyridin-2-ylmethoxy)phenyl)-1H-phenanthro[9,10-d]imidazole (5)

A mixture of 9,10-phenanthrenequinone (0.42 g, 2 mmol), ammonium acetate (1.5 g, 2 mmol) was suspended in a solution of ethanol (30 mL) and dichloromethane (3 mL). The suspension was heated to reflux until all solids were dissolved and then cooled to room temperature. 2-(Pyridin-2-ylmethoxy)benzaldehyde (0.426 g, 2 mmol) and a drop of acetic acid were added to the mixture which was again heated to reflux for 2 h, cooled, and the crude product was filtered and washed with ethanol to afford 0.62 g of compound **5** (0.62 g, 78%) as a yellow solid. <sup>1</sup>H NMR (400 MHz, CDCl<sub>3</sub>) δ ppm: 12.93 (s, 1H), 9.00 (dt, *J* = 4.35, 1.54 Hz, 1H), 8.82 (dd, *J* = 7.96, 1.12 Hz, 1H), 8.76 (dt, *J* = 7.79, 1.75 Hz, 2H), 8.71 (d, *J* = 8.33 Hz, 1H), 8.37 (dd, *J* = 7.95, 1.13 Hz, 1H), 7.80 (td, *J* = 7.70, 1.77 Hz, 1H), 7.66-7.76 (m, 2H), 7.62 (m, 2H), 7.41 (d, *J* = 7.59 Hz, 3H), 7.23 (td, *J* = 7.82, 1.07 Hz, 1H), 7.18 (d, *J* = 8.24 Hz, 1H), 5.49 (s, 2H). <sup>13</sup>C NMR (100 MHz, CDCl<sub>3</sub>) δ ppm: 155.7294, 155.1141, 149.8573, 147.1222, 137.0730, 130.1922, 129.8430, 128.2731, 126.7600, 124.9979, 123.3831, 122.3351, 121.5181, 119.3915, 112.6859, 70.4111. HRMS (ESI<sup>+</sup>, Fig. S11) calc. for C<sub>27</sub>H<sub>19</sub>N<sub>3</sub>O (M + H<sup>+</sup>) 402.1601, found 402.1599.



Scheme 1. Syntheses of chemosensor **3** and reference compound **5**.

## Results and discussion

The synthesis of compound **3** is shown in Scheme 1. Briefly, **2** was prepared by an elimination reaction between 2-(chloromethyl)pyridine hydrochloride and **1**, which was synthesized according to a previously reported procedure. Compound **3** was obtained in fair yield by heating a mixture of 9,10-phenanthrenequinone and **2** to reflux in acetonitrile for 6 h. All compounds were characterized by  $^1\text{H}$  NMR,  $^{13}\text{C}$  NMR, and MS (SI, Fig. S1-S13). A similar compound 2-(2-(pyridin-2-ylmethoxy)phenyl)-1H-phenanthro[9,10-d]imidazole **5**, without the cyanophenyl group found in **3**, was synthesized in good yield with the same procedure, but using the commercially available 2-(pyridin-2-ylmethoxy)benzaldehyde as a starting material. Comparison of the fluorescence emission spectra of **3** and **5** showed a very weak fluorescence emission peak at 393 nm for **3** which can be attributed to the ICT from the phenanthro[9,10-d]imidazole moiety to the CN group.

### UV-Vis absorption studies

With compound **3** in hand, first absorption and fluorescence properties were investigated in DMF-water (1:1, v/v) with HEPES buffer solution (pH = 7.0) under excitation at 300 nm.<sup>28</sup> The solution of **3** was colourless and exhibited two mild absorption bands at 329 nm and 364 nm (Fig. S14). The bands increased upon gradual addition of an aqueous solution of  $\text{CrCl}_3$  (0–8 equiv.), which could be attributed to an electron density increase of the imidazole moiety due to inhibition of ICT arising from metal chelation. After binding  $\text{Cr}^{3+}$ , the solution turned from colourless to light-blue immediately upon exposure to UV light ( $\lambda_{\text{em}} = 365$  nm). Such a dramatic colour change under UV light could make compound **3** a sensitive turn-on chemosensor for  $\text{Cr}^{3+}$  detection.

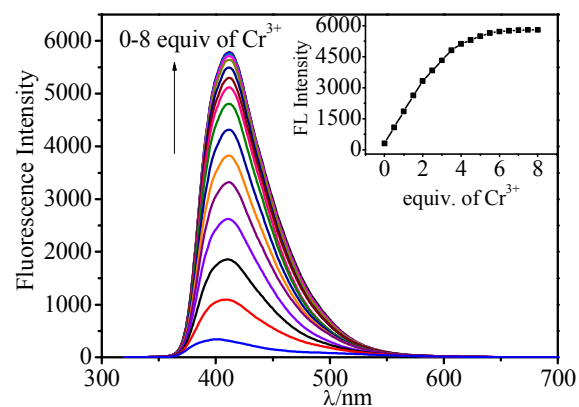


**Fig. 1.** Change of emission spectra of sensor **3** (20  $\mu\text{M}$ ) upon the gradual addition of  $\text{Cr}^{3+}$  (0 to 8 equiv.). Inset: the plot of fluorescent emission intensity at 412 nm as a function of  $\text{Cr}^{3+}$  concentration ( $\lambda_{\text{em}} = 300$  nm).

### Fluorescence emission studies

A weak fluorescence emission band for **3** at 393 nm in the absence of  $\text{Cr}^{3+}$  was observed in a DMF-water solution (1/1, v/v, 20 mM HEPES buffer at pH = 7.0) upon excitation at 300 nm (Fig. 1). This band could be assigned to a strong intra-molecular charge transfer (ICT) band transition. The fluorescence quantum yield was evaluated as being 0.127 with anthracene as a reference. Addition of 0.5 equiv. of  $\text{Cr}^{3+}$  led to a strong emission at 412 nm. This red shift from 393 nm to 412 nm can be attributed to the internal

charge transfer (ICT) as found previously.<sup>29</sup> The emission intensity reached its maximum on adding 8 equiv. of  $\text{Cr}^{3+}$ , which increased by 15 fold as compared with that of free **3**. The quantum yield of  $\text{3-Cr}^{3+}$  was found to be 0.917, a ca. 7-fold enhancement on the free sensor.

Furthermore, sensor **3** exhibited a good linear relationship between the intensity at 412 nm and  $\text{Cr}^{3+}$  concentration with a  $R^2$  value of 0.996 (shown in Fig. 2). Based on this, the detection limit was evaluated to be  $1.72 \times 10^{-8} \text{ M}^{-1}$  (Table S1), which is 180-fold lower than the maximum level (0.96  $\mu\text{M}$ ) of total chromium in drinking water permitted by the WHO.<sup>30</sup> Indeed, this detection limit was found to be superior to all but two of the reported  $\text{Cr}^{3+}$  sensors in the literatures (Table S2).<sup>21,31</sup> A Job plot indicated a 1:1 binding stoichiometry with a maximum emission change observed at a mole ratio of 1:1 for sensor **3** and  $\text{Cr}^{3+}$  (Fig. 3). The association constant ( $K_a$ ) of  $4.44 \times 10^3 \text{ M}^{-1}$  was calculated from a Benesi-Hildebrand plot (Fig. 4) using data obtained from a UV-Vis titration. This value was found to be comparable to most turn-on sensors reported in the literature (Table S2).

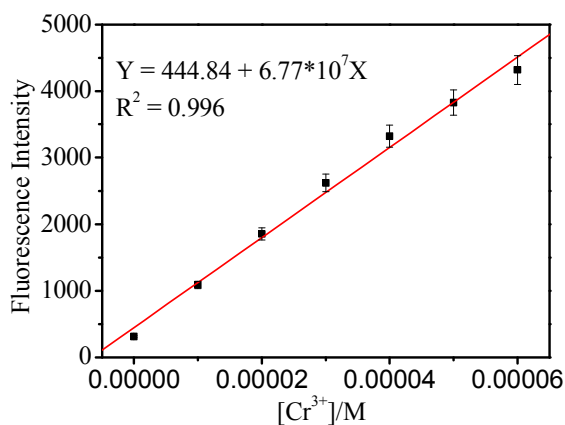


**Fig. 2.** Fluorescence intensity at 412 nm of **3** versus increasing concentrations of  $\text{Cr}^{3+}$  ( $\text{Cr}^{3+}$  concentration: 0, 0.5, 1, 1.5, 2, 2.5, 3 equiv.,  $\lambda_{\text{ex}} = 300$  nm). Each spectrum was acquired 5 minutes after  $\text{Cr}^{3+}$  addition at room temperature.

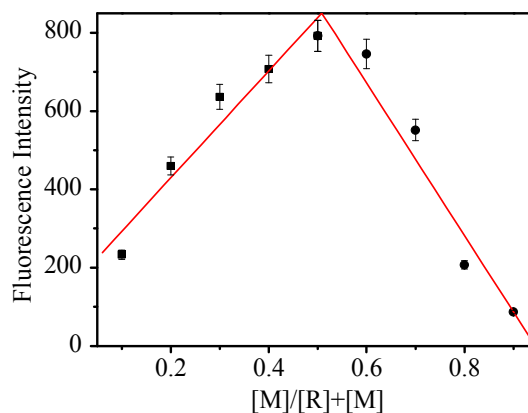


**Fig. 3.** Job plot for the complexation of  $\text{Cr}^{3+}$  ion with **3** determined by UV-vis method (at 412 nm,  $\lambda_{\text{ex}} = 300$  nm). Total concentration of **3** and  $\text{Cr}^{3+}$  ions is 20  $\mu\text{M}$ .

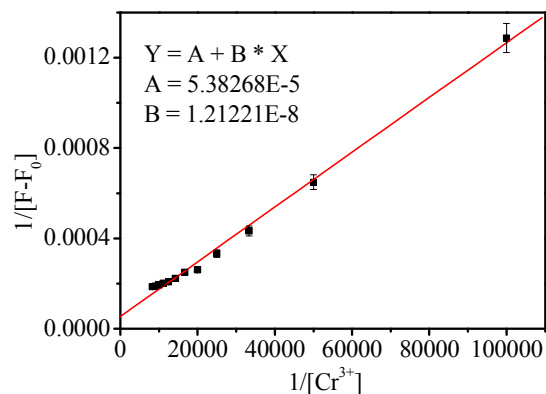


**Fig. 4.** Benesi-Hilderbrand plot of **3** with  $\text{Cr}^{3+}$  ( $F$  is the fluorescence intensity of **3** in the presence of  $\text{Cr}^{3+}$ ,  $F_0$  is the fluorescence intensity of free **3**).

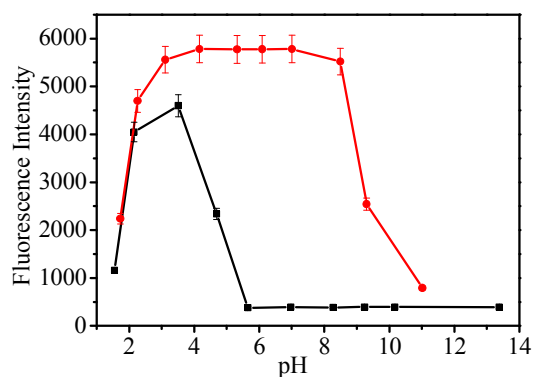


**Fig. 5.** Fluorescence response at 393 nm for chemosensor **3** (black line, 20  $\mu\text{M}$ ,  $\lambda_{\text{ex}} = 300 \text{ nm}$ ) and at 412 nm for complex  $\text{3-Cr}^{3+}$  (red line) as a function of pH in DMF- $\text{H}_2\text{O}$  (1:1, v/v); the pH was adjusted using 1 M aqueous solutions of HCl or NaOH.

#### pH range

The influence of pH on fluorescence intensity of chemosensor **3** in the absence and presence of  $\text{Cr}^{3+}$  was investigated at various pH values in the DMF- $\text{H}_2\text{O}$  (1:1, v/v) solution. The fluorescence response at varying pH is shown in Fig. 5, with maximum emissions at 393 nm and 412 nm for the free sensor and the complex  $\text{3-Cr}^{3+}$ , respectively. The emission at 390 nm was observed when the solution of the free chemosensor **3** was in a more acidic environment ( $\text{pH} < 4.0$ ) ( $\lambda_{\text{ex}} = 360 \text{ nm}$ ). This is most likely because the imidazole and pyridine groups become protonated at low pH. In contrast, the fluorescence intensity of  $\text{3-Cr}^{3+}$  was sharply quenched at pH 8.5 with the addition of base. This could likely be attributed to a release of  $\text{Cr}^{3+}$  from the complex at high pH which gave the free chemosensor in which ICT is on. This good fluorescence response of **3** toward  $\text{Cr}^{3+}$  in the 6.5-8.5 pH range demonstrates that it can be used as a sensitive chemosensor under physiological conditions.

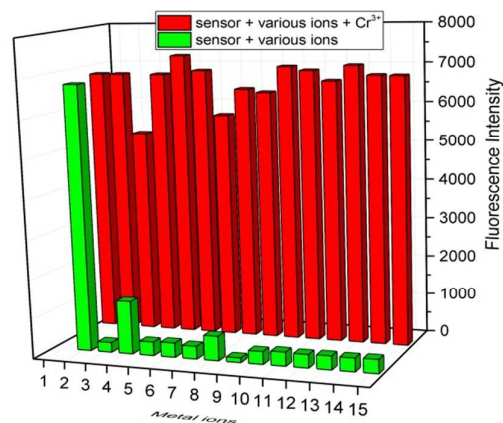


**Fig. 6.** Fluorescence intensity of **3** (20  $\mu\text{M}$ ) in DMF- $\text{H}_2\text{O}$  (1:1, v/v) at 412 nm after 8 equiv. of various cations (blue bars) and those after further addition of 8 equiv. of  $\text{Cr}^{3+}$  (red bars). 1, Blank; 2,  $\text{Cr}^{3+}$ ; 3,  $\text{Ag}^+$ ; 4,  $\text{Al}^{3+}$ ; 5,  $\text{Ba}^{2+}$ ; 6,  $\text{Cd}^{2+}$ ; 7,  $\text{Cu}^{2+}$ ; 8,  $\text{Fe}^{3+}$ ; 9,  $\text{Hg}^{2+}$ ; 10,  $\text{K}^+$ ; 11,  $\text{Mn}^{2+}$ ; 12,  $\text{Na}^+$ ; 13,  $\text{Ni}^{2+}$ ; 14,  $\text{Pb}^{2+}$ ; 15,  $\text{Zn}^{2+}$ .  $\lambda_{\text{ex}} = 300 \text{ nm}$ .



**Fig. 7.** Colour change of **3** upon interaction with tested cations (top: under natural light; bottom: under UV light). From left to right: Blank,  $\text{Cr}^{3+}$ ,  $\text{Ag}^+$ ,  $\text{Al}^{3+}$ ,  $\text{Ba}^{2+}$ ,  $\text{Cd}^{2+}$ ,  $\text{Cu}^{2+}$ ,  $\text{Fe}^{3+}$ ,  $\text{Hg}^{2+}$ ,  $\text{K}^+$ ,  $\text{Mn}^{2+}$ ,  $\text{Na}^+$ ,  $\text{Ni}^{2+}$ ,  $\text{Pb}^{2+}$ ,  $\text{Zn}^{2+}$ .

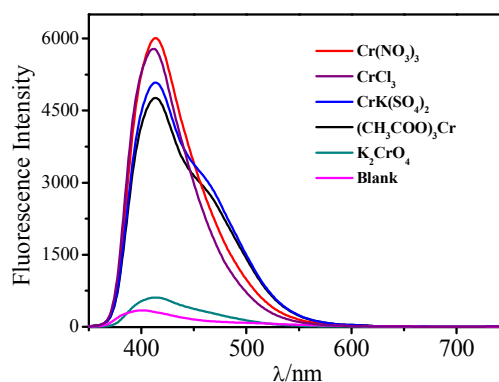


**Fig. 8.** Fluorescence response of **3** (20  $\mu\text{M}$ ) with 10 equiv. of various chromium salts in DMF- $\text{H}_2\text{O}$  (1:1, v/v, HEPES, 20 mM, pH 7.0,  $\lambda_{\text{ex}} = 300 \text{ nm}$ ).

#### Competition and response time

Competition experiments to study the selectivity of chemosensor **3** with various metal ions were performed and the respective fluorescence



intensities are displayed in Fig. 6. When the titration was conducted in a DMF-H<sub>2</sub>O solution (1/1, v/v, HEPES 20 mM, pH 7.0), only Cr<sup>3+</sup> induced a significant fluorescence enhancement although Al<sup>3+</sup> and Fe<sup>3+</sup> induced a weak fluorescence change. However, the colour change from colourless to blue was only observed for Cr<sup>3+</sup> and not for Al<sup>3+</sup> and Fe<sup>3+</sup>. Other competitive metal ions including Na<sup>+</sup>, K<sup>+</sup>, Ag<sup>+</sup>, Hg<sup>2+</sup>, Cd<sup>2+</sup>, Cu<sup>2+</sup>, Ni<sup>2+</sup>, Li<sup>+</sup>, Ni<sup>2+</sup>, Ba<sup>2+</sup>, Mn<sup>2+</sup>, Zn<sup>2+</sup>, Fe<sup>3+</sup> and Pb<sup>2+</sup> did not show any obvious absorbance and fluorescence emission change, even at a concentration of 50 equiv. of metal ions under physiological conditions (Fig. 7). This remarkable colour change and fluorescence response clearly demonstrated the good selectivity of sensor **3** for Cr<sup>3+</sup>. Competition titration also revealed that sensor **3** demonstrated a high affinity for trivalent cations with a strong positive charge (Fig. 6). Similar results were observed by other research groups where rhodamine derivatives were used as probe molecules.<sup>32-34</sup> The effect of choice of anion on the fluorescent properties of sensor **3** was also explored (Fig. 8). In each case the choice of anion did not have a significant effect although Cr(NO<sub>3</sub>)<sub>3</sub> gave a slightly higher intensity to the other Cr<sup>3+</sup> salts. This is likely due to the difference between the binding ability and steric hindrance of the anions used in this study. K<sub>2</sub>CrO<sub>4</sub> also demonstrated only a negligible response. The addition of Cr<sup>3+</sup> to a mixture of **3** and the other potentially competitive metal ions (40 equiv.) mentioned above in a DMF-H<sub>2</sub>O (1:1) solution, led to a significant fluorescence intensity enhancement (Fig. 9). These observations demonstrated that sensor **3** could be used as an efficient fluorescence chemosensor for Cr<sup>3+</sup> ion with high selectivity.

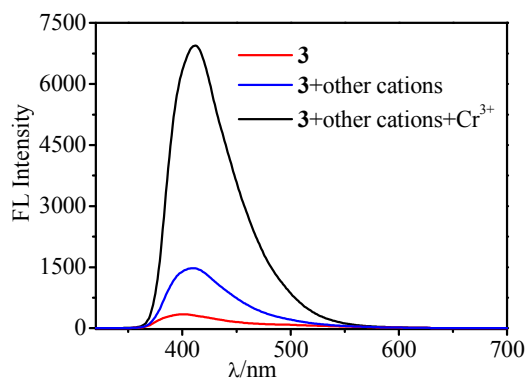


**Fig. 9.** Fluorescence intensity of **3** (20 μM) in the absence of metal ions (red curve), and presence of 8 equiv. of all kinds of competitive metal ions (blue curve) in DMF-water (1:1, v/v, pH 7.0, λ<sub>ex</sub> = 300 nm). The black curve represents the addition of CrCl<sub>3</sub> to the above mixture.

Response time is a fundamental parameter for most reaction-based chemosensors, and the kinetic profile of the reaction of chemosensor **3** and Cr<sup>3+</sup> at room temperature was examined (Fig. 10). The fluorescence emission reached equilibrium within 10 seconds of injection of Cr<sup>3+</sup> into a solution of chemosensor **3** (DMF-H<sub>2</sub>O, 1:1, v/v, HEPES 10 mM, pH 7.0). The emission intensity hardly changed over the subsequent 120 s, which confirmed that **3**-Cr<sup>3+</sup> was stable. These results implied that our proposed chemosensor would provide a rapid analytical method for the detection of Cr<sup>3+</sup>. Cr<sup>3+</sup> in river water and tap water samples was determined by sensor **3** to examine the applicability of the proposed method. The satisfactory recovery results were summarized in Table 1.

**Table 1** Determination of Cr<sup>3+</sup> with sensor **3** in samples (n = 5).

Sample	Cr <sup>3+</sup> added (μM)	Cr <sup>3+</sup> found (μM)	Recovery (%)
Tap water	0	Not detected	0
	10	9.88	98.8
	40	39.6	99.2
River water	0	Not detected	0
	10	9.84	98.4
	40	39.3	98.3

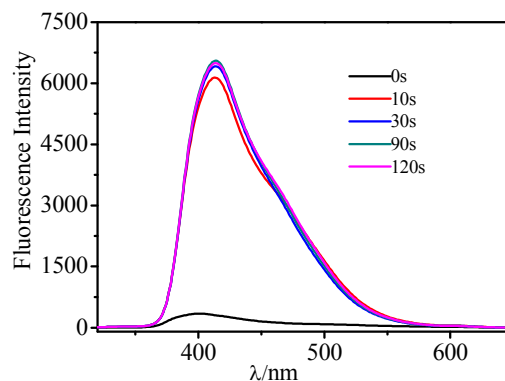
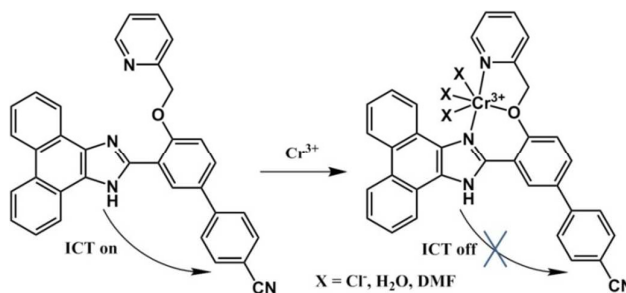


**Fig. 10.** Effect of time on the fluorescence intensity of **3** (20 μM) in the presence of 8 equiv. of CrCl<sub>3</sub> in DMF-H<sub>2</sub>O (1:1, v/v) at pH 7.0 (HEPES 20 mM).



**Scheme 2.** Proposed mechanism for enhanced fluorescence response of **3** upon addition of CrCl<sub>3</sub>.

### Fluorescence recognition mechanism

It is well known that fluorescent turn-on chemosensors are preferable due to their highly selectivity, sensitivity and ease of observation<sup>35-37</sup>. The enhanced fluorescence response of chemosensor **3** when binding Cr<sup>3+</sup> could be attributed to an interference of both intra-molecular charge transfer (ICT) and chelation energy transfer (CHEF). To investigate the mechanism of ICT, compound **5** was designed and synthesized and the fluorescence intensity of **5** in the absence and presence of Cr<sup>3+</sup> was performed (Fig. S15). As expected, there was no ICT observed for reference **5** due to the lack of an electron withdrawing group. Upon binding to Cr<sup>3+</sup>, a small enhancement in fluorescence intensity was found as well as a peak shift from 393 nm to 408 nm, likely attributable to CHEF. A proposed mechanism for the enhanced fluorescence response of **3** is depicted in scheme 2. In contrast to **5**, the free chemosensor **3** in a DMF/H<sub>2</sub>O (1/1, v/v) solution shows a very weak fluorescence emission at 393 nm, likely because electrons can transition

from the highest occupied molecular orbital (HOMO) to the lowest unoccupied molecular orbital (LUMO), which make ICT in sensor **3**. When the imidazole and pyridyl groups of sensor **3** chelate to  $\text{Cr}^{3+}$ , the redox potential of the donor is raised so that the relevant HOMO lowers in energy compared to that of the fluorophore. Electrons in the excited state cannot therefore return to the ground state and the intra-molecular charge transfer is switched off due to the lack of conjugation in the phenanthroimidazole moiety. Furthermore coordination likely causes a locally excited band so that the emission band at 393 nm shifts bathochromically and a very large enhancement of fluorescence at 412 nm is observed as a consequence.

### Theoretical study

To get insight into the optical response of **3** to  $\text{Cr}^{3+}$ , The geometries of **3**, **5**, and **3**- $\text{CrCl}_3$  in DMF solution were optimized by density functional theory (DFT) with the B3LYP functional and the LANL2DZ basis set for Cr and 6-31G\*\* basis set for the other atoms (Fig. S16), respectively. The polarizable continuum model (PCM) was implemented to consider the solvent effect. The calculation results showed that the ground state of **3**- $\text{CrCl}_3$  is a quartet state and the spin density is mainly distributed on the Cr atom (see Fig. S17). It can be seen that the flexibility of **3** would be decreased due to the coordination with  $\text{Cr}^{3+}$ .

Based on the optimized geometries, the singlet excited states for compounds **3** and **5** in water and DMF solutions were obtained by time-dependent DFT (TDDFT) at the B3LYP/6-31G\*\* level in combination with the PCM. For both **3** and **5**, the  $S_1$  state arises from the HOMO  $\rightarrow$  LUMO transition. As shown in Fig. S18, the HOMO and LUMO for **5** are almost delocalized on the whole molecule, leading to a large overlap between HOMO and LUMO and thus a strong oscillator for the  $S_1$  state. The HOMO of **3** is similar to that of **5**, but the LUMO is mainly localized on the additional electron-withdrawing group. Consequently, the  $S_1$  state of **3** has an obvious charge transfer state and a much smaller oscillator (see Table S3), which is fully consistent with our experiments.

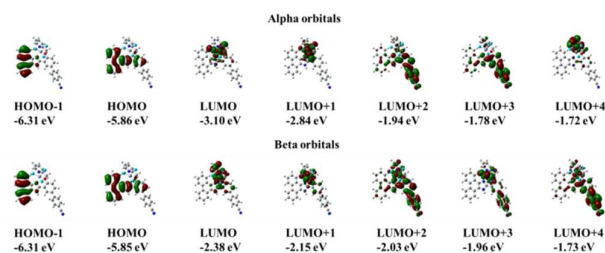


**Fig. 11.** DFT-calculated frontier molecular orbitals for **3**- $\text{CrCl}_3$  in DMF solution.

At present, it is still a challenge to accurately calculate the excited states of high spin for an open-shell system. Here, we will qualitatively discuss the excited states of **3**- $\text{CrCl}_3$ . As seen from the experimental data, the emission wavelengths of compounds **3** and **3**- $\text{Cr}^{3+}$  are quite similar. Since the energy gap between the HOMO and LUMO+2 of **3**- $\text{CrCl}_3$  is closest to that between the HOMO and LUMO of **3**, apparently the fluorescent state of **3**- $\text{Cr}^{3+}$  arises from the HOMO  $\rightarrow$  LUMO+2 transition. Fig. 11 demonstrates that the HOMO of **3**- $\text{CrCl}_3$  is similar to that of **3** while the LUMO of **3**- $\text{CrCl}_3$  becomes much more extended to the whole conjugated backbone. Thus, the fluorescent state of **3**- $\text{Cr}^{3+}$  can have a stronger oscillator with respect to **3**, which agrees with the experimental observation.

### Conclusions

In summary, we have successfully designed and synthesized a simple fluorescent chemosensor based on the combination of ICT and CHEF mechanisms. The experimental results clearly indicated that chemosensor **3** was a highly sensitive and selective chemosensor for  $\text{Cr}^{3+}$  in a DMF- $\text{H}_2\text{O}$  (1:1, v/v, pH = 7.0) solution. Remarkably, the probe exhibited a fast turn-on fluorescence response to  $\text{Cr}^{3+}$  within 10 seconds. The fluorescence enhancement with high selectivity and sensitivity was attributed to ICT and CHEF. It was found that the probe had a detection limit of  $1.72 \times 10^{-8} \text{ M}^{-1}$  and worked within a pH range of 6.5-8.5 demonstrating its value for practical application in physiological systems. However, the short emission wavelength of 412 nm of **3** limits its application. These excellent fluorescence results allow us to design new chemosensors with a long emission wavelength through removing the electron-withdrawing groups or changing the CN group to one electron donating group and the related investigation is fully under way.

### Acknowledgements

We thank the national Natural Science Foundation of China (grant No. 21101074), Shandong Provincial Natural Science Foundation of China (grant No. ZR2013BQ009) and the Doctor's Foundation of University of Jinan (Grant No. XBS1320) for funding.

### Notes and references

- 1 K. W. Huang, H. Yang, Z. G. Zhou, M. X. Yu, F. Y. Li, X. Gao, T. Yi and C. H. Huang, *Org. Lett.*, 2008, **10**, 2557-2560.
- 2 X. H. Li, X. H. Gao, W. Shi and H. M. Ma, *Chem. Rev.*, 2014, **114**, 590-659.
- 3 D. W. Domaille, E. L. Que and C. J. Chang, *Nat. Chem. Biol.*, 2008, **4**, 168-175.
- 4 M. Wang, X. M. Liu, H. Z. Lu, H. M. Wang and Z. H. Qin, *ACS Appl. Mater. Interfaces*, 2015, **7**, 1284-1289.
- 5 R. McRae, P. Bagchi, S. Sumalekshmy and C. J. Fahrni, *Chem. Rev.*, 2009, **109**, 4780-4827.
- 6 S. K. Panda, *J. Plant Physiol.*, 2007, **164**, 1419-1428.
- 7 S. Latva, J. Jokiniemi, S. Peraniemi and M. Ahlgren, *J. Anal. At. Spectrom.*, 2003, **18**, 84-86.
- 8 R. Bencheikh-Latmani, A. Obratsova, M. R. Mackey, M. H. Ellisman and B. M. Tebo, *Environ. Sci. Technol.*, 2006, **41**, 214-220.
- 9 J. Kovacic, P. Babula, B. Klejduš and J. Hedbavny, *J. Agric. Food Chem.*, 2013, **61**, 7864-7873.
- 10 D. A. Brose and B. R. James, *Environ. Sci. Technol.*, 2010, **44**, 9438-9444.
- 11 Y. Li, C. Chen, B. Li, J. Sun, J. Wang, Y. Gao, Y. Zhao and Z. Chai, *J. Anal. At. Spectrom.*, 2006, **21**, 94-96.
- 12 Y.-J. Gong, X.-B. Zhang, C.-C. Zhang, A.-L. Luo, T. Fu, W.-H. Tan, G.-L. Shen and R.-Q. Yu, *Anal. Chem.*, 2012, **84**, 10777-10784.
- 13 J. Sun, J. Zhang and Y. D. Jin, *J. Mater. Chem. C*, 2013, **1**, 138-143.
- 14 X. M. Huang, C. H. Fan, Z. Wang, X. F. Zhan, M. S. Pei and Z. L. Lu, *Inorg. Chem. Commun.*, 2015, **57**, 62-65.
- 15 J. P. Zhang, L. Zhang, Y. L. Wei, J. B. Chao, S. B. Wang, S. M. Shuang, Z. W. Cai and C. Dong, *Anal. Methods*, 2013, **5**, 5549-5554.
- 16 K. Rurack, M. Kollmannsberger, U. Resch-Genger and J. Daub, *J.*

- Am. Chem. Soc.*, 2000, **122**, 968-969.
- 17 M. Zhang, M. X. Yu, F. Y. Li, M. W. Zhu, M. Y. Li, Y. H. Gao, L. Li, Z. Q. Liu, J. P. Zhang, D. Q. Zhang, T. Yi and C. H. Huang, *J. Am. Chem. Soc.*, 2007, **129**, 10322-10323.
- 18 M. Zhao, L. Ma, M. Zhang, W. Cao, L. Yang and L.-J. Ma, *Spectrochim. Acta Part A: Mol. Mol. Biomol. Spectrosc.*, 2013, **116**, 460-465.
- 19 H. M. Wu, P. Zhou, J. Wang, L. Zhao and C. Y. Duan, *New J. Chem.*, 2009, **33**, 653-658.
- 20 A. N. Kursunlu, E. Sahin and E. Güler, *RSC Adv.*, 2015, **5**, 5951-5957.
- 21 F. Z. Hu, B. Z. Zheng, D. M. Wang, M. P. Liu, J. Du and D. Xiao, *Analyst*, 2014, **139**, 3607-3613.
- 22 Y. Wan, Q. J. Guo, X. F. Wang and A. D. Xia, *Anal. Chim. Acta*, 2010, **665**, 215-220.
- 23 J. Y. Jung, S. J. Han, J. Chun, C. Lee and J. Yoon, *Dyes Pigm.*, 2012, **94**, 423-426.
- 24 D. Liu, T. Pang, K. Ma, W. Jiang and X. Bao, *RSC Adv.*, 2014, **4**, 2563-2567.
- 25 J. Mao, L. Wang, W. Dou, X. Tang, Y. Yan and W. Liu, *Org. Lett.*, 2009, **9**, 4567-4570.
- 26 J. Zhang, C. Zhong, X. J. Zhu, H.-L. Tam, K.-F. Li, K.-W. Cheah, W.-Y. Wong, W.-K. Wong and R. A. Jones, *Polyhedron*, 2013, **49**, 121-128.
- 27 J. M. Doshi, D. Tian and C. Xing, *J. Med. Chem.*, 2006, **49**, 7731-7739.
- 28 S. Angupillai, J.-Y. Hwang, J.-Y. Lee and B. A. Rao, *Sens. Actuators B*, 2015, **214**, 101-110.
- 29 S. Goswami, K. Aich, S. Das, C. D. Mukhopadhyay, D. Sarhar and T. K. Mondal, *Dalton Trans.*, 2015, **44**, 5763-5770.
- 30 WHO, *Guidelines for Drinking-Water Quality*, World Health Organization, 4th edn, Geneva, Switzerland, 2011.
- 31 P. Mahato, S. Saha, E. Suresh, R. D. Liddo, P. P. Parnigotto, M. T. Conconi, M. K. Kesharwani, B. Ganguly and A. Das, *Inorg. Chem.*, 2012, **51**, 1769-1777.
- 32 Y. Xiang and A. Tong, *Org. Lett.*, 2006, **8**, 1549-1552.
- 33 V. Dujols, F. Ford and A. W. Czarnik, *J. Am. Chem. Soc.*, 1997, **119**, 7386-7387.
- 34 J. H. Huang, Y. F. Xu and X. H. Qian, *Dalton Trans.*, 2014, **43**, 5983-5989.
- 35 Y. Xu, W. Yang, J. Shao, W. Zhou, W. Zhu and J. Xie, *RSC Adv.*, 2014, **4**, 15400-15405.
- 36 M. Kaur, P. Kaur, V. Dhuna, S. Singh and K. Singh, *Dalton Trans.*, 2014, **43**, 5707-5712.
- 37 C.-Y. Li, X.-F. Kong, Y.-F. Li, C. Weng, J.-L. Tang, D. Liu and W.-G. Zhu, *Anal Chim Acta*, 2014, **824**, 71-77.